PROCEEDINGS, Fourtieth Workshop on Geothermal Reservoir Engineering
Stanford University, Stanford, California, January 26-28, 2015
SGP-TR-204

Reservoir Response to Thermal and High-Pressure Well Stimulation Efforts at Raft River, Idaho

Mitchell Plummer, Hai Huang, Robert Podgorney, Jacob Bradford, Joseph Moore

Idaho Falls National Laboratory, MS 2107, 2525 Fremont St, Idaho Falls, ID, 83415-2107

Mitchell.Plummer@inl.gov

Keywords: Well stimulation, injectivity, enhanced geothermal systems

ABSTRACT

An injection stimulation test begun at the Raft River geothermal reservoir in June, 2013 has produced a wealth of data describing well and reservoir response via high-resolution temperature logging and distributed temperature sensing, seismic monitoring, periodic borehole televiewer logging, periodic stepped flow rate tests and tracer injections before and after stimulation efforts. The hydraulic response demonstrates continually increasing injectivity, reflected in varying flow rate response to nearly constant injection pressure, but features of the hydraulic response provide information about different characteristics of the reservoir. Changes in injectivity immediately following high-flow rate tests suggest that hydro shearing has altered the near-well permeability structure, while pressure response during those tests indicates that near-well permeability is relatively homogeneous and low but that the well is near, but not well connected to, a zone of higher transmissivity. Long-term changes in injectivity are believed to reflect propagation of the injection cooling front through low permeability zones. Two dimensional flow and heat transport simulations are used to demonstrate how the timescale of pressure response may relate to length scales of permeability distribution.

INTRODUCTION

Whether to increase productivity of existing hydrothermal reservoirs, or to engineer new geothermal reservoirs, methods of stimulating wells to increase productivity are essential to expansion of geothermal energy. To provide a detailed study of well response to stimulation on the edges of an active hydrogeothermal system, the Department of Energy Geothermal Technology Program is sponsoring an Enhanced Geothermal System study at the Raft River Geothermal Reservoir in southern, Idaho. An existing well at that location, well RRG-9, was drilled to the depth of other productive reservoir wells but proved to have injectivity too low for economic use as either a production well or cold water injection well. The project involves application of a series of stimulation methods to well RRG-9 ST-1 and detailed monitoring of the well to better understand reservoir response to stimulation. The stimulation methods include long-term cold water injection at a variety of flow rates and injection temperatures, aimed at improving permeability by cooling and contraction of the fractured rock host formation, followed by high-pressure injections designed to alter permeability via application of fluid pressures that exceed the fracture gradient. Methods of monitoring the reservoir include high-resolution temperature logging within the well at all times, via distributed temperature sensing, seismic monitoring, periodic borehole televiewer logging, periodic stepped flow rate tests and tracer injections before and after stimulation efforts. In this paper, we discuss recent data and analysis from the thermal and high-pressure stimulation efforts in well RRG-9, and implications for the nature of the fractured reservoir and stimulation efforts in general.

BACKGROUND

Raft River Geothermal Area

The Raft River geothermal reservoir is located in Cassia County Idaho approximately six miles north of the Utah/Idaho border near the town of Malta (Figure 1). This site was heavily studied by the U.S. Department of Energy from 1975 to 1982 and was the testing site of the first commercial scale binary (isobutene) cycle geothermal power plant in the world. The site is currently owned and operated by U.S. Geothermal and is producing power from a 13-MW (nominal) binary isopentane power system.

The Raft River geothermal site is located near the southern end of the Raft River north-south trending valley (Figure 1). This valley is characterized by high-angle normal faulting, low-angle faulting emplacing younger over older rocks, moderate plutonism, and the presence of discontinuous metamorphic terrains (Allman et al., 1982). Beneath the surface alluvium, the Salt Lake Formation is a thick (~1200 meter) poorly consolidated deposit consisting of siltstone and sandstone. Underlying this formation is a 150-meter thickness of metasediments, consisting of sub-units of schist and quartzite. The base rock is a Precambrian adamellite. The western side of the valley has been down-dropped along listric faults in the Bridge and Horse Well Fault zones through the Salt Lake Formation. These faults dip 60 to 80 degrees to the east at the surface and become nearly horizontal in the Tertiary Sediments and may have produced many near vertical open fractures at the base of the sediments. Movement along of these faults is believed to have created vertical fractures in the base of the Salt Lake Formation and in the underlying Precambrian metasediments that are responsible for the high well yields in the geothermal field (Allman et al., 1982; Dolenc et al., 1981).

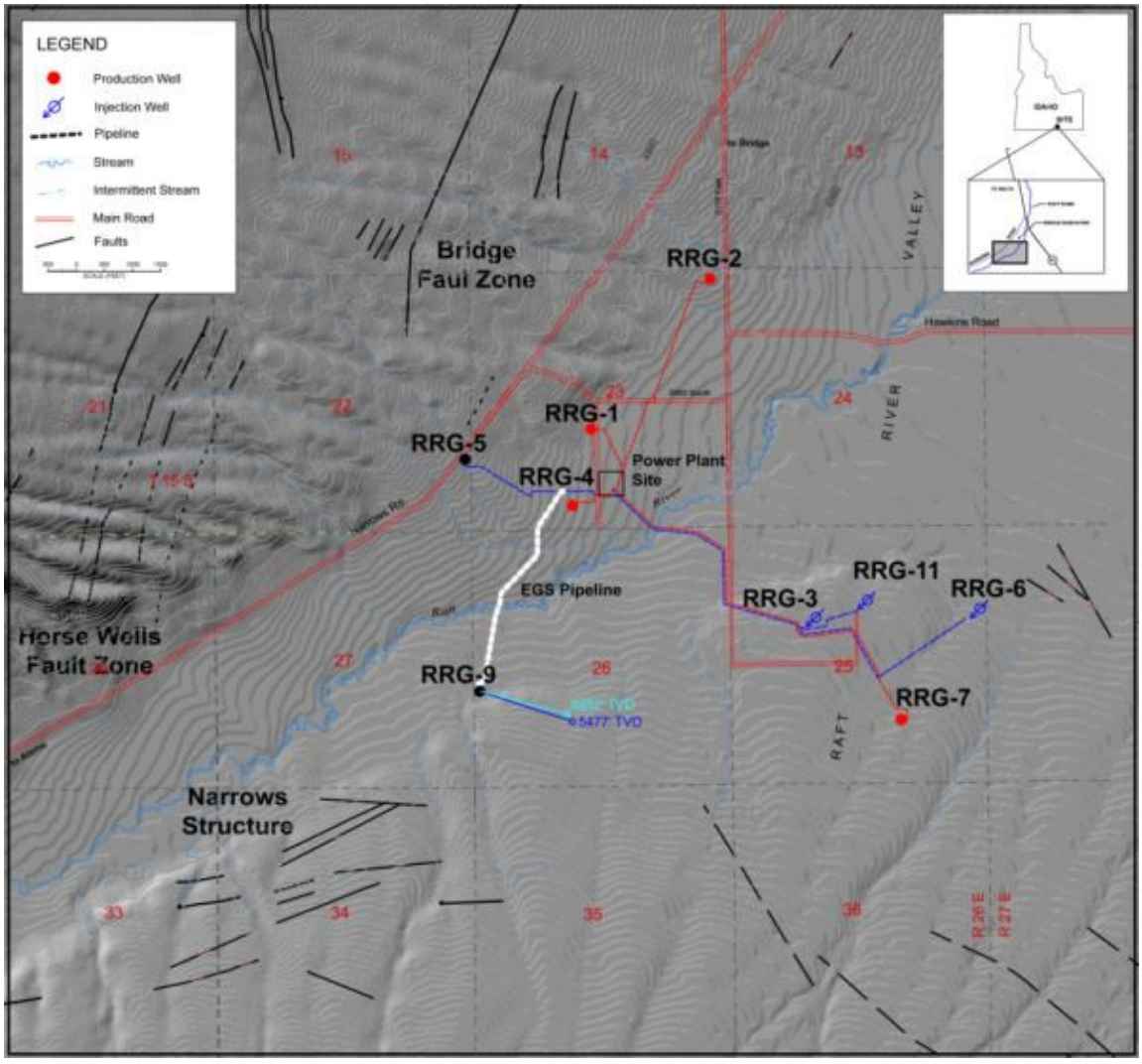

Figure 1. Map showing well locations and infrastructure within the Raft River geothermal field and major fault zones.

Well Stimulation

A multi-phase stimulation program is in progress at well RRG-9 ST-1 (

Table 1). Phase I of the stimulation began on June 13, 2013 with injection from the power plant at a temperature of about 39 °C, pressure of 275 psig and flow rate of approximately 40 gpm. That injection continued until August 20, 2013, and was immediately followed by a stepped rate injection test, on August 22, 2013, prior to initiation of the next phase of injection. That test was aimed at detecting differences in reservoir behavior as compared to a similar, February 24, 2012 test conducted well before Phase I of the stimulation. In phase II, two positive displacement plunger type pumps were used to increase the injection pressure and flow rate for about one month. The highest rate achieved was 261 gpm at a pressure of 809 psig. During this time, fluid from the cooler water well was injected in a series of steps of increasing flow rate. The pumps were then removed and plant injection resumed on September 25, 2013 and continued until March 30, 2014. Flow rates and wellhead pressures during the latter period were approximately 122-133 gpm at 272-281 psi. Between April 1 and April 3, 2014, high pressure injection testing via a series of steps of constant injection rate was conducted, to attempt to increase permeability via hydroshearing of existing fractures in the vicinity of the well.

Table 1. Injection history during the cold-water injection stimulation phases at well RRG-9.

Source	Booster Pump(s)	Time Period	Flow Rate (gpm)	Average WHP (psi)	Average Fluid Temperature (°C)
Plant Injectate	No	13-Jun to 20-Aug	43	280	39
Plant Injectate	No	23-Aug to 30-Aug	141	540	40
Plant Injectate	Yes	1-Sep to 8-Sep	261	809	46
Cold Well Water	Yes	12-Sep to 16-Sep	254	743	12
Cold Well Water	Yes	16-Sep to 24-Sep	191	522	13
Plant Injectate	No	25-Sep to 2-Dec	122	272	30
Plant Injectate	No	3-Dec to 30-Mar	133	281	27
Plant Injectate	No	4-April to present (30-April 2014)	133	281	27

STIMULATION RESPONSE

The reservoir's response to the stimulation efforts is evident in several features of the long-term flow and pressure record (Figure 2), which each provide information about a different timescale or different aspect of behavior. At the shortest timescale, distinct jumps in injectivity occur following the two high pressure injection tests in August 2013 and April 2014. These jumps suggest that near-well permeability increases have occurred via hydro shearing of fractures or mitigation of well skin effects developed during drilling.

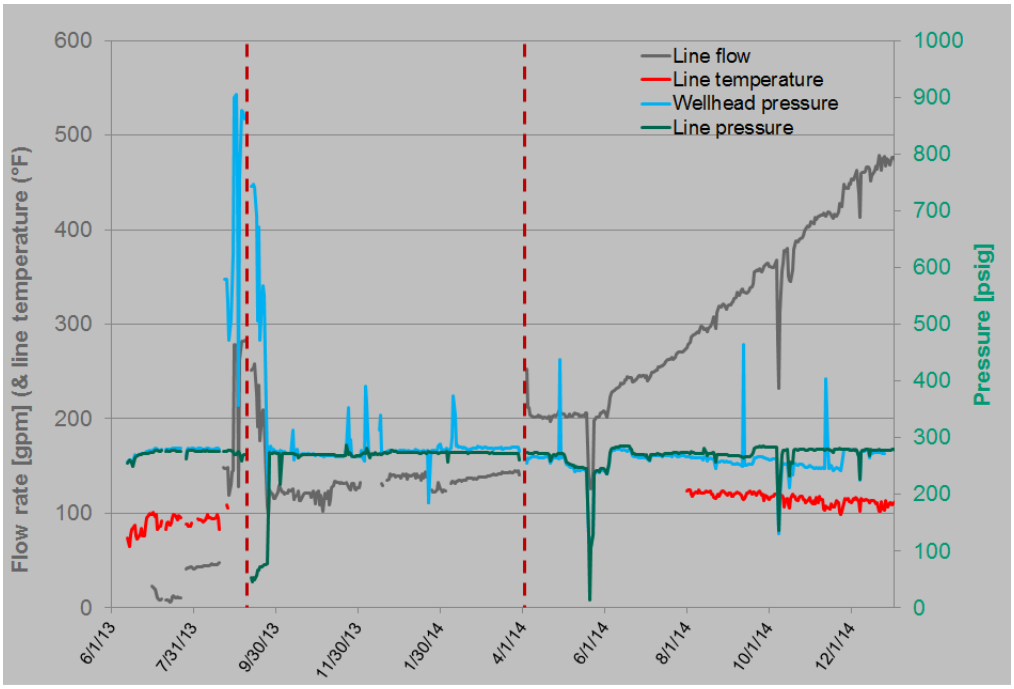

Figure 2. Daily averages of data collected from well RRG-9 during the stimulation project. Red dashed lines indicate high pressure injection test periods.

At a similarly short timescale, pressure response curves during the stepped rate pressure tests have a shape that suggests a radial flow regime (Figure 3). We used the commercial package Aqtesolv (Duffield, 2007) to test a variety of reservoir response models, including, for example, models incorporating vertical and horizontal fractures, aquifers with leakage from surrounding formations, partial penetrating wells and wellbore storage. Results demonstrated that the Theis-Hantush type curve, or similar models assuming essentially uniform radial flow, provided substantially better fit than more heterogeneous models. Our estimates of transmissivity and storativity for the fracture network, and further analyses of response during stepped changes in flow rate are, therefore, based on the Theis-Hantush model of well response to pumping.

Because each step in those tests lasts for less than hour, the affected radial extent is relatively small. The distance over which fluid pressure increases are felt depends largely on hydraulic diffusivity of the fractured rock, which depends, in turn, on the thickness of the fractured rock reservoir, its compressibility and permeability. The constant flow rate tests consistently suggest a permeability on the order of 1E-13 m^2 to 1E-14 m^2. Assuming a total storativity between 2E-6 m Pa^{-1} and 2E-8 m Pa^{-1}, a 1/e - fold change in Δp, relative to the Δp measured at the well, would extend to between 5 and 10 m from the injection point.

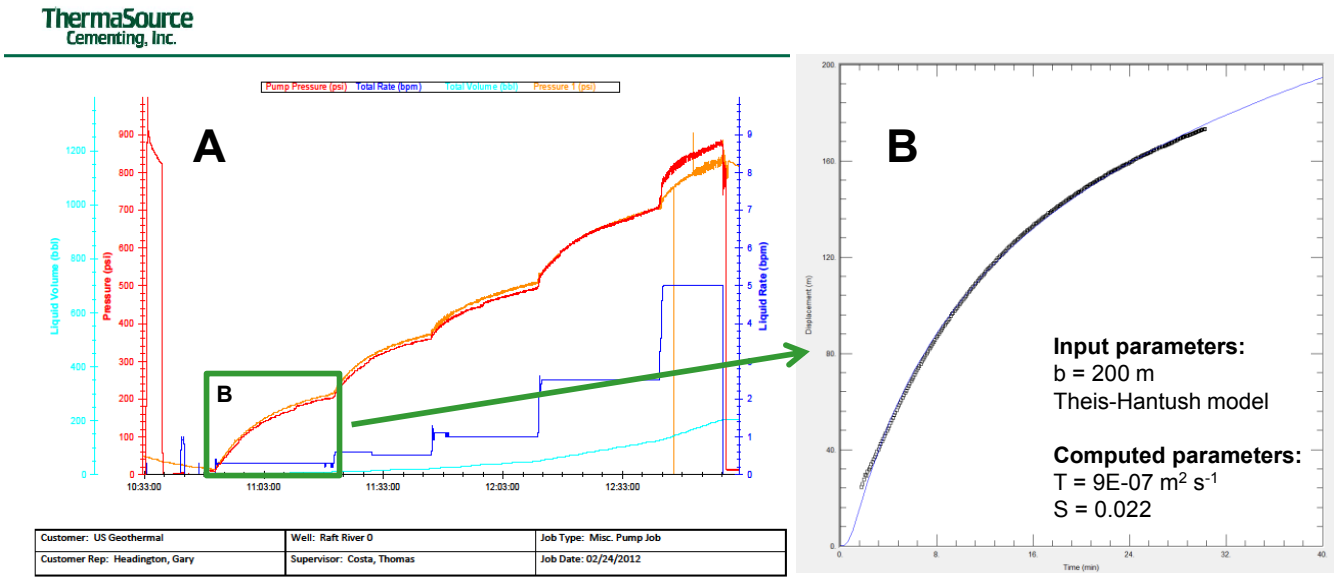

Figure 3. (A) February 24, 2012 step rate test conditions from 10:33 to 13:00. The dark blue and light blue lines represent the liquid pumping rate and cumulative volume respectively. The red and orange lines are the measured pressure. (B) Best-fit Theis-Hantush curve solution and parameters from analysis using Aqtesolv, from first step of data in A.

According to the radial flow model implied by the above analysis, pressure would continue to increase during constant injection, but at a rate that diminishes with time. This is contrary, however, to what is observed in the long-term pressure response. Figure 4 illustrates well response during a 12-day period in early September, during which the flow rate changed dramatically on several occasions, and which evidences long-term pressure response to initially steady pressure. At 3.5 days in this record, the well returns to steady injection after a period of greatly reduced injection rate, and at 8 days in, the well recovers to zero gage pressure after a long period of steady flow and pressure. In each case, the pressure appears to reach steady state in approximately 18 hours.

The most complete data set for analysis during that period is the pressure response to resumption of a constant rate injection at 287 gpm from a hydrostatic condition, shown in Figure 5. Again, the early time data suggests a radial flow regime, as demonstrated by the excellent fit to a Theis solution. At 200 minutes, however, there is a strong departure from that curve, and the rate of pressure increase after that point is much slower than would occur in a uniform radial flow scenario. This suggests heterogeneity in the reservoir that provides net greater diffusivity at a relatively short distance from the well, whether that is a change to a more spherical flow regime or interception of a more permeable zone in one or more directions from the well.

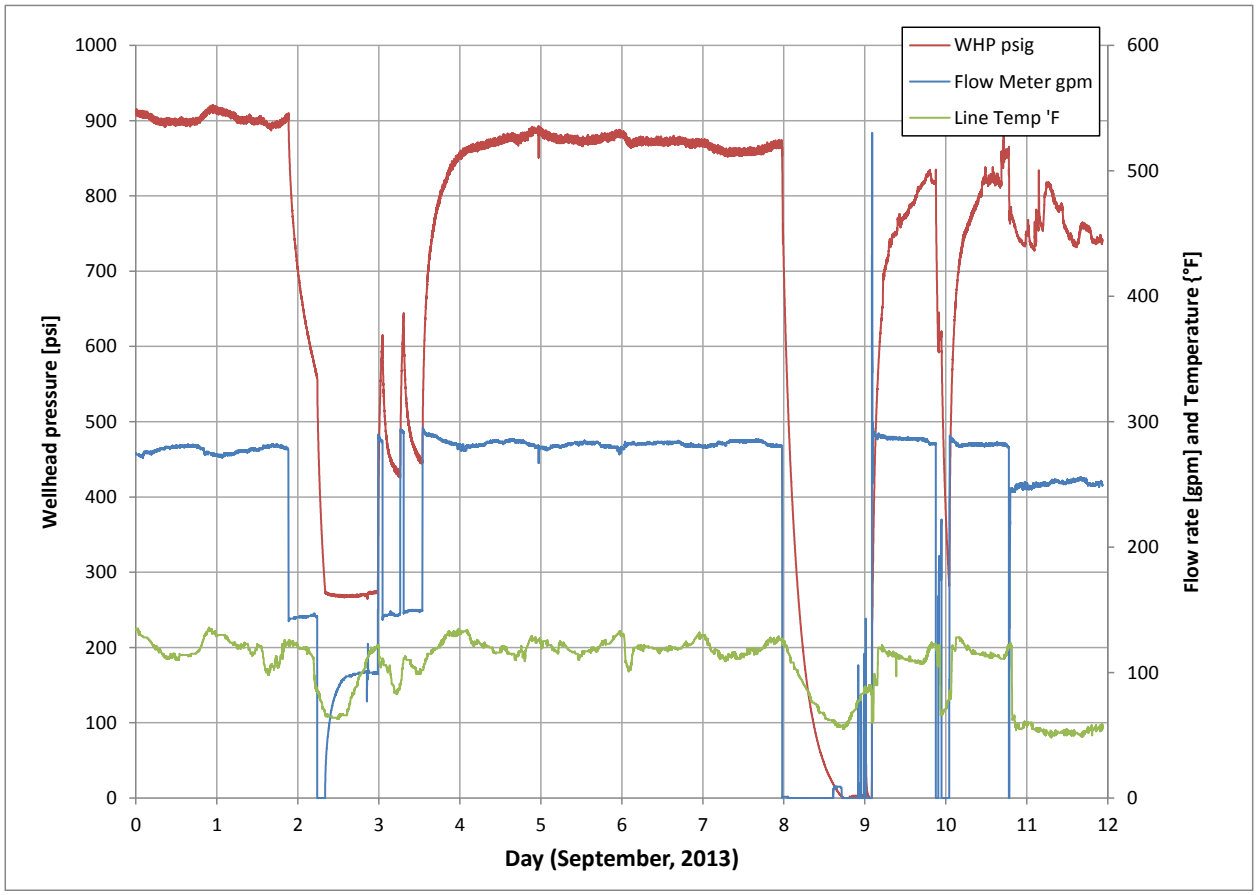

Figure 4. Wellhead pressure, injection rate, and injection line temperature during a 12-day period in early September, 2013, evidencing long-term pressure response during two ~1-day periods following a large change in flow rate.

To illustrate how a model with heterogeneity can better reproduce the observed pressure response, we show results of analytical (1D radial flow) solution that provides a reasonable fit to the data. To estimate the distance to the hypothesized region of greater transmissivity, we introduce a boundary into the radial flow solution, and vary the distance to it as a fitting parameter. In this model, we assume a relatively low hydraulic diffusivity in the near-well region, in order to reproduce the slow rise of pressure at early time. That low diffusivity, which results in a slow rate of pressure increase away from the well implies, in turn, that the more transmissive region, that causes the inflection at 200 minutes, is relatively near the well. In this case, placing a constant head boundary at a distance of 0.7 meters creates a pressure response curve that reproduces the observed response. In a 2D flow model, inclusion of simple heterogeneity would produce a similar response.

The remaining notable features in the pressure response to stimulation injections are the gradual increases in injectivity (evident as increases in flow rate at constant pressure) that occur during most of the ~1.5-year project. The gradual increase is generally slow but a marked acceleration in rate occurred at the beginning of June, 2014, following a temporary shutdown. While it is difficult to explain the coincidence of changes in these gradual increases in injectivity, such changes are consistent with injectivity increases expected to result from the migration of the cooling front away from the well and the consequent rock contraction and fracture dilation, in a heterogeneous reservoir.

To illustrate how relatively simple heterogeneities can reproduce the general nature of the apparent injectivity response to thermal stimulation, we constructed a plan-view 2D finite element model solving equations of flow and heat transport. To reproduce short timescale pressure observed at RRG-9, the model is based on hydraulic properties derived from the short term stepped rate tests (Table 2). The model is comprised of three rectangular zones, with permeability increasing by an order of magnitude across zonal boundaries, from bottom to top (Figure 6). Left hand, top and bottom sides of the domain are no-flow boundaries for mass and heat, while the right hand boundary is fixed pressure, representing a distant zone of effectively constant hydraulic head and temperature. An injection well is located at the left boundary, just below the bottom of zone 2, at a distance of approximately one meter. The proximity of that boundary, combined with the contrast in hydraulic diffusivity makes pressure response to injectivity behave essentially as observed at well RRG-9 during the September 9, 2013 restart (Figure 5).

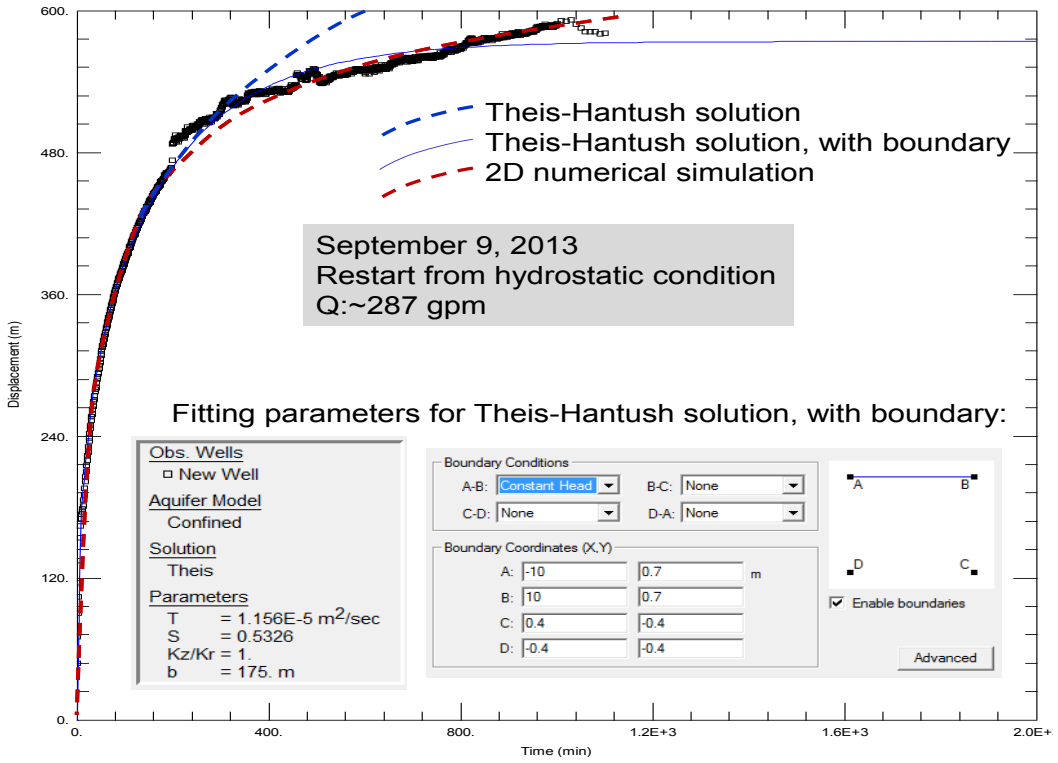

Figure 5. (A) September 9, 2013 injection startup, at constant injection rate of ~287 gpm. Symbols and lines represent, respectively, data and fitted curves.

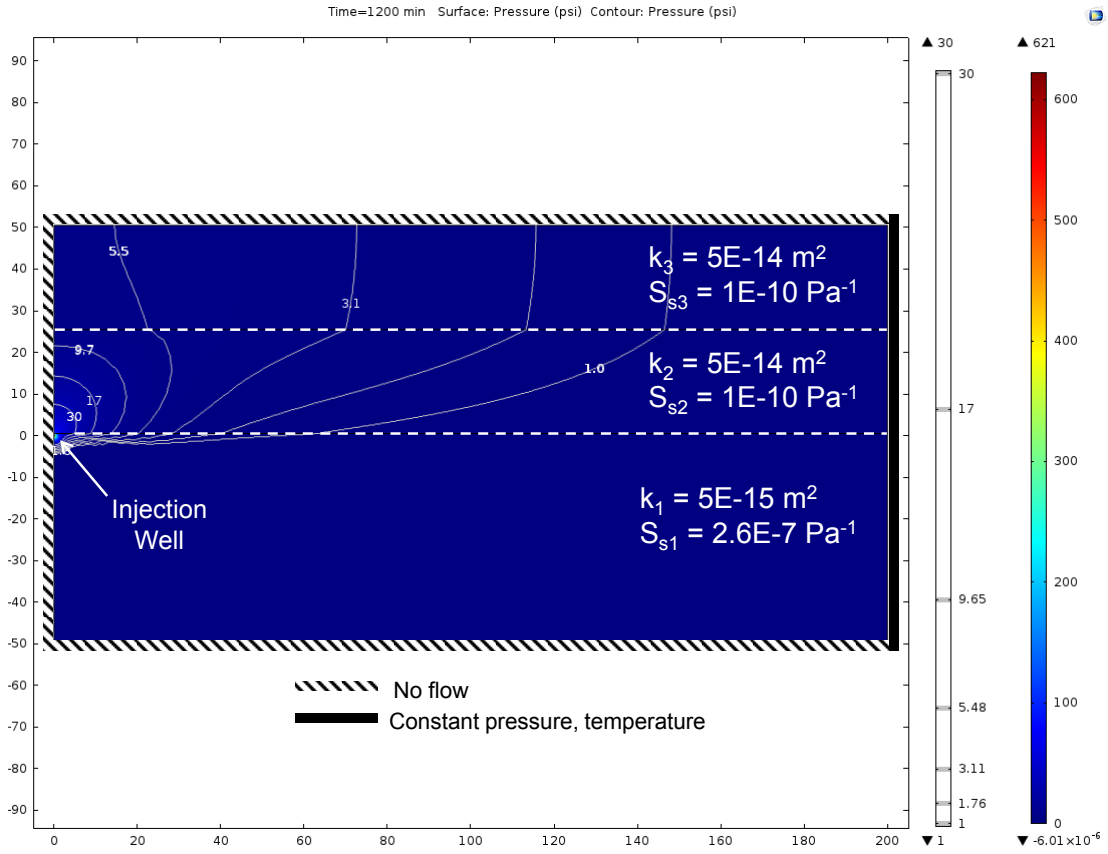

Figure 6. Schematic of finite element simulation domain described in the text, with pressure distribution developed following 1200 minutes of pumping at the injection rate described in Table 2.

The arrangement of rectangular domains may be considered to represent a large fault zone with increasing permeability in the ordinate direction, with the top and bottom of the domains representing adjacent zones of very low transmissivity. In this arrangement, as the cooling front due to cold water injection progresses through regions of lower permeability toward regions of higher permeability, the connection to higher permeability zones increases and higher injectivity should result. The timescale over which that would occur is defined by the timescale for heat transport, which depends on a number of parameters, the most uncertain of which is probably fracture distribution. An equilibrium heat transport model can provide a reasonable indicator of the rate at which the cooling front will propagate from the well through the constriction.

Again, because we focus here on demonstrating possible scenarios that could reproduce observed pressure response at Raft River, we apply an constant injection pressure in long-term flow simulations equivalent to the injection field pressure supplied by the powerplant (270 psi). Assuming a porosity of 1%, and applying a simple linear feedback between pressure and permeability, the evolution of temperature and permeability in the simulated reservoir then evolves as shown in Figure 7 (A-C). The consequent increases in permeability (Figure 7 (D-F) then result in a variably increasing flow rate, as summarized in Figure 8. The flow rate has marked inflections at 5 and 50 days that coincide with times (Figure 7) at which the cooling front has essentially reached, first, zone 2 and, second, zone 3. The rate of increase of injectivity depends both on the rate of propagation of the thermal front and the magnitude of the increase in the permeability.

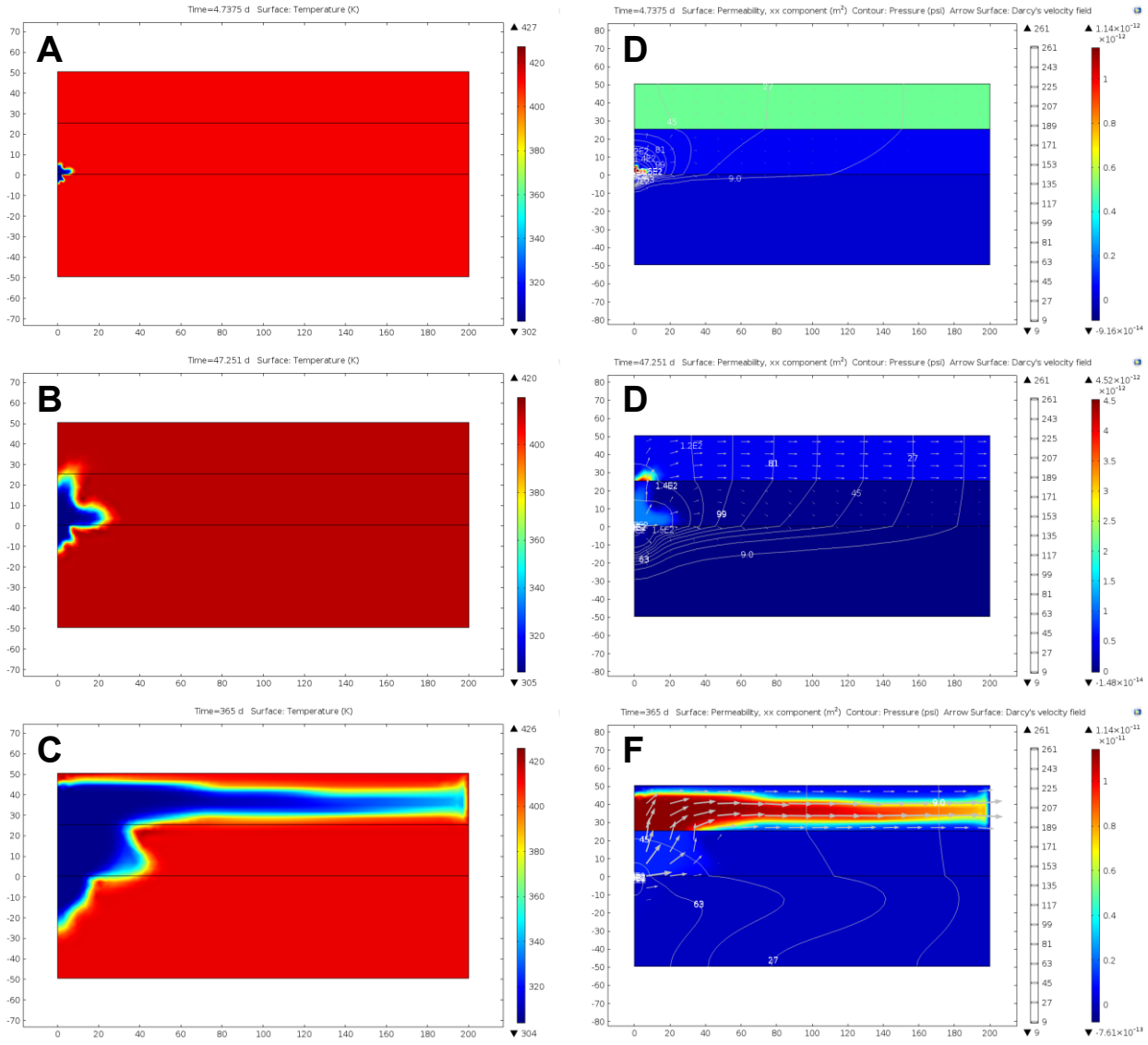

Figure 7. Evolution of temperature (A,B,C) and permeability (D,E,F) under the simulated conditions described in the text. Plots are shown for snapshots at approximately 5, 50 and 365 days of injection.

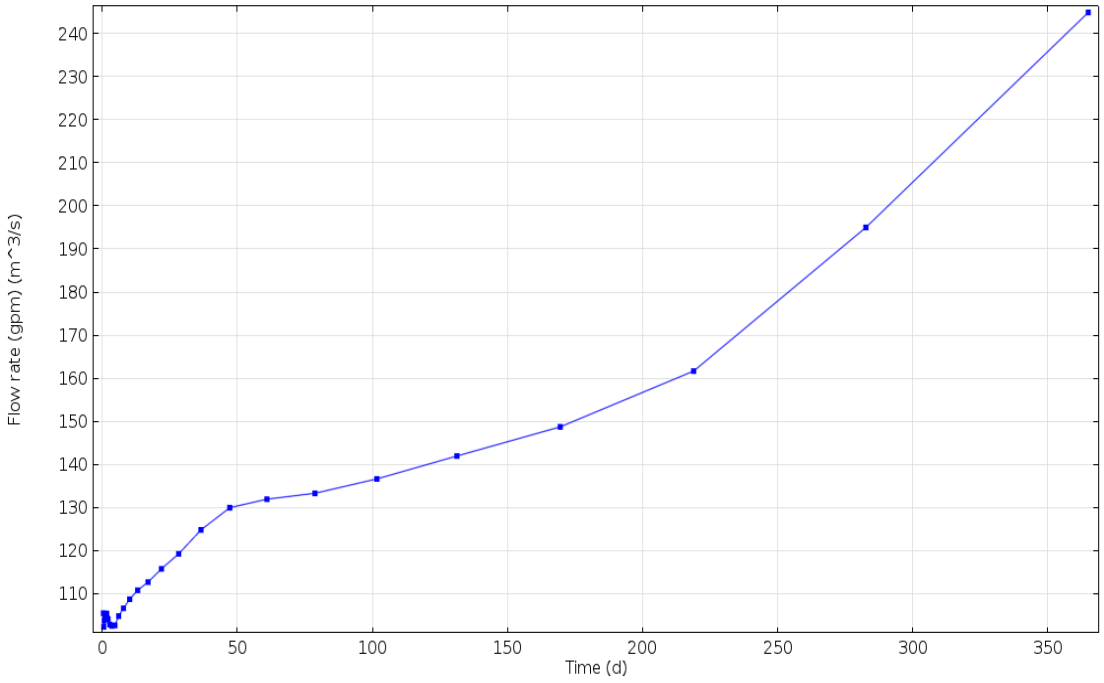

Figure 8. Flow rate response to constant pressure injection for the simulation shown in Figure 7.

Table 2. Parameters used in finite element simulations described in the text

Parameters

Name	Expression	Value	Description
r1_ht	50	50	Rectangle 1 height
r1_w	r1_ht*4	200	Rectangle 1 width
r_well	9[in]/2	0.1143 m	Radius of well
r_disk	0.4[m]	0.4 m	Radius of horizontal fracture intersecting well
p_init	0[psi]	0 Pa	Pressure, initial
p_distal	0[psi]	0 Pa	Pressure, distal boundaries
p_inj	270[psi]	1.8616E6 Pa	Pressure, injection
T_inj	90[degF]	305.37 K	Temperature, injection
T_res	140[degC]	413.15 K	Temperature, reservoir
epsilon_ht	0.001	0.001	Porosity, for heat transport
b	200[m]	200 m	Thickness of reservoir
Q_well	170[gal/min]	0.010725 m^3/s	Flow rate to well
q_wellsection	Q_well/(2*pi*r_well*b)	7.4671E-5 m/s	Well face velocity
kappa_1	5e-15[m^2]	5.0000E-15 m^2	Permeability, zone 1
kappa_2	5e-14[m^2]	5.0000E-14 m^2	Permeability, zone 2
kappa_3	5e-13[m^2]	5.0000E-13 m^2	Permeability, zone 3
Ss_1	2.6e-7[1/Pa]	2.6000E-7 1/Pa	Specific storage, zone 1
Ss_2	1e-10[1/Pa]	1.0000E-10 1/Pa	Specific storage, zone 2
Ss_3	1e-10[1/Pa]	1.0000E-10 1/Pa	Specific storage, zone 3
eta	2E-4[Pa*s]	2.0000E-4 Pa·s	Dynamic viscosity, water
Diff_1	kappa_1/(Ss_1*eta)	9.6154E-5 m^2/s	Diffusivity, zone 1
Diff_2	kappa_2/(Ss_2*eta)	2.5 m^2/s	Diffusivity, zone 2
Diff_3	kappa_3/(Ss_3*eta)	25 m^2/s	Diffusivity, zone 3

CONCLUSIONS

One of the primary measures of reservoir response to the injection stimulation project begun at the Raft River geothermal facility in 2013 is the flow rate and pressure response of the injection well. That provides indirect information about the hydraulic properties of the reservoir and, thus, the general nature of fracture distribution and different features of the flow and pressure response curves provide information about different length scales. The hydraulic response thus provides a means of testing hypotheses about the hydraulic properties distribution in the reservoir and, therefore, the hypothesized geologic model of faults and other structures that control permeability.

Because hydraulic diffusivity is much greater than thermal diffusivity, short term variations, such as responses to short-term stepped rate tests, represent pressure-induced effects, while slow gradual changes in injectivity likely represent the propagation of the injection cooling front through hydraulic constrictions. The analysis and simulations here are intended to demonstrate how various features of the long-term hydraulic record can be interpreted, and what constraints they place on geologic interpretation, rather than as a best-estimate of hydraulic conditions the subject injection well.

REFERENCES

Allman, D.W., Tullis, J.A, Dolenc, M.R., Thurow, T.L. and Skiba P.A. (1982), “Raft River Monitor Well Potentiometric Head Responses and Water Quality as Related to the Conceptual Ground-Water Flow System”, EG&G Idaho Inc. Technical Report (EGG-2215), Vol. II, prepared for the US Department of Energy, Idaho Operations Office.

Bradford, J., M. Ohren, W. Osborn, J. McLennan, J. Moore, and R. Podgorney, Thermal Stimulation and Injectivity Testing at Raft River, ID EGS Site, Proceedings, Thirty-Ninth Workshop on Geothermal Reservoir Engineering, Stanford University, Stanford, California, February 24-26, 2014.

Dolenc, M.R., Hull, L.C., Mizell, S.A., Russell, B.F., Skiba, P.A., Strawn, J.A., and Tullis J.A. (1981), “River River Geoscience Case Study”, EG&G Idaho Inc. Technical Report (EGG-2125), Vol. I, prepared for the US Department of Energy, Idaho Operations Office.

Duffield, G.M., 2007. AQTESOLV for Windows Version 4.5 User's Guide, HydroSOLVE, Inc., Reston, VA.

Kruseman, G.P.; de Ridder, N.A. (1990). Analysis and Evaluation of Pumping Test Data (Second ed.). Wageningen, The Netherlands: International Institute for Land Reclamation and Improvement. ISBN 90-70754-20-7.

Williams, P. L., K, L, Pierce, D, H, McIntire, and P. W. Schmidt, 1974. Preliminary geologic map of the southern Raft River area, U.S.G.S. Open File Report, 1:24,000.